Received: 29 July 2019 | Revised: 24 September 2019 | Accepted: 14 November 2019

DOI: 10.1002/pro6.1078

ORIGINAL ARTICLE

Effect of colony-stimulating factor-1 receptor overexpression on the growth of nasopharyngeal carcinoma xenografts in nude mice and its mechanism of action

Zenan Chen[1,2] | **Yanrong Hao**[1]

[1]Cancer Center, People's Hospital of Guangxi Zhuang Autonomous Region, Guangxi, China

[2]Hubei Provincial Hospital of Traditional Chinese Medicine, Hubei, China

Correspondence
Yanrong Hao, Cancer Center, People's Hospital of Guangxi Zhuang Autonomous Region, Guangxi 530000, P.R. China.
Email: 554805917@qq.com

Funding information
The present study was supported by the Key projects of Department of Public Health of Guangxi Zhuang Autonomous (grant no. 2010037) and the Natural Science Foundation of China (grant no. 81260348).

Abstract

Objectives: Although nasopharyngeal carcinoma (NPC) is sensitive to radiotherapy, local recurrence and distant metastasis still occur in a proportion of patients due to radioresistance. Our previous research confirmed that colony-stimulating factor-1 receptor (CSF-1R) promotes the proliferation, migration, and invasion of 6-10B cells through the phosphoinositide 3-kinase (PI3K) pathway *in vitro*. The objective of the present study was to investigate the effects of colony-stimulating factor-1 receptor (CSF-1R) on proliferation, apoptosis, and autophagy in the human nasopharyngeal carcinoma 6-10B cell line *in vivo*, and the possible underlying mechanisms.

Methods: A virus carrying the CSF-1R gene was transfected into 6-10B cells by lentiviral transfection. A nasopharyngeal carcinoma xenograft model in nude mice was established. Ultimately, the protein expression of proliferation-, apoptosis-, autophagy-, and signaling-related proteins, such as cyclin D1, B-cell lymphoma 2 (Bcl-2), Bcl-2-associated X protein, beclin 1, microtubule-associated protein 1 light chain 3 alpha, sequestosome 1, mechanistic target of rapamycin kinase, PI3K, and protein kinase B (Akt/PKB), in tumor tissues were detected by western blot analysis.

Results: High levels of CSF-1R were expressed in the stably transfected 6-10B cells, while CSF-1R promoted the growth of 6-10B cells *in vivo*. Cyclin D1, Bcl-2, microtubule-associated protein 1 light chain 3 alpha, and beclin 1 were upregulated, while Bcl-2-associated X protein and sequestosome 1 were downregulated. Furthermore, the expression of PI3K, phospho-Akt, Akt, and mechanistic target of rapamycin kinase were upregulated.

Conclusions: CSF-1R overexpression promotes proliferation, reduces apoptosis, and induces autophagy in 6-10B cells *in vivo*, and the corresponding mechanism might be executed through activation of the PI3K/Akt pathway.

KEYWORDS

B-cell lymphoma 2, B-cell lymphoma 2-associated X protein, beclin 1, colony-stimulating factor-1 receptor, nasopharyngeal carcinoma, sequestosome 1

1 | INTRODUCTION

Nasopharyngeal carcinoma (NPC) is a highly prevalent malignancy with a significant geographic incidence, and approximately 80% of NPCs occur in southern China and southeastern Asia.[1,2] Although NPC is usually sensitive to radiotherapy, local recurrence and distant metastasis still occur in a proportion of patients due to radioresistance.[3] Previously, we have compared gene expression profiles between 12 radioresistant NPC patients and eight radiosensitive patients using DNA chip technology, and observed that the colony-stimulating

factor-1 receptor (CSF-1R) showed a distinct difference between the two groups. Its expression in tissues of radiation-resistant patients was higher than that in radiation-sensitive patients.[4] Therefore, we hypothesize that CSF-1R might induce radiotherapy resistance in NPC patients, and hence there is an urgent need to decipher the molecular mechanism of CSF-1R in NPC to formulate better treatment plans.

CSF-1R is a 972 amino acid long single-chain transmembrane glycoprotein belonging to the tyrosine kinase receptor family. CSF-1R is produced in the osteoblasts, bone marrow stromal cells, endothelial cells, fibroblasts, and epithelial cells. It is also widely expressed during tumor progression, thus playing a key role in the process.[5] *In vivo*, CSF-1R, and CSF-1 are phosphorylated upon binding to activate their phosphokinase domain, which then activates the mononuclear macrophage system to promote tumor growth, neovascularization, and extracellular matrix decomposition. CSF-1R thus enables tumor cells to drive tumor development. Studies have also shown that CSF-1R directly affects tumor cells,[6] and this could be associated with CSF-1R being overexpressed in individual tumors.[7–9] Hence, CSF-1R detected in circulating blood is identified as a tumor marker in certain malignancies. However, there is little evidence on the effect of CSF-1R on NPC.

Our previous *in vitro* studies confirmed the role of CSF-1R in promoting the proliferation, migration, and invasion of 6-10B cells through the phosphoinositide 3-kinase (PI3K) pathway.[10] Furthermore, in this study, we developed a nude mouse model of NPC, and sequentially evaluated the expression of CSF-1R and other proliferation-, invasion-, apoptosis-, autophagy-, and PI3K/protein kinase B (Akt) pathway-related factors in the xenograft model. We sought to determine the molecular mechanism of CSF-1R in the progression of NPC through *in vivo* experiments to unravel the possible causes of radiotherapy resistance seen in NPC cases. CSF-1R might serve as a potential candidate for NPC gene therapy, and we hope to provide experimental evidence to identify new molecular targets for NPC treatment in the future.

2 | METHODS

2.1 | Cell culture and animals

The NPC cell line 6-10B was obtained from Sun Yat-Sen University Cancer Center (State Key Laboratory of Oncology in South China, Guangzhou, China). Cells were cultured in RPMI-1640 medium (Thermo Fisher Scientific, Waltham, MA, USA) containing 10% fetal bovine serum (Gibco; Thermo Fisher Scientific,), and incubated in a humidified (37°C, 5% CO_2) incubator. The medium was changed every 2 days.

A total of 15 (5 per group) BALB/c-nu mice were provided by the Laboratory Animal Center of Guangxi Medical University (Nanning, China). The mice were 4–5 weeks old and weighed 18 g. They were bred in laminar-flow cabinets, and housed at constant humidity and temperature (25–28°C) following the standard guidelines. All animal experiments were reviewed and approved by the Institutional Animal Care and Use Committee of the People's Hospital of Guangxi Zhuang Autonomous Region.

2.2 | Generation of CSF-1R lentiviral vector constructs and transfection procedures

To generate the CSF-1R overexpression vectors, lentiviral vectors carrying the enhanced green fluorescent protein gene was used (constructed by Shanghai GeneChem, Shanghai, China). CSF-1R (NM 005211; GeneChem) was transformed into the GV358 vector (GeneChem) using the Clon Express II One Step Cloning Kit (Vazyme Biotech, Nanjing, China). The constructs thus generated were further transfected into HEK293T cells with lentiviral packaging vectors using Lipofectamine 2000 (Invitrogen, Carlsbad, CA, USA). The generated lentiviruses (recombinant with single copy CSF-1R gene or control vector) were used to infect the 6-10B cell lines following 2D transfection protocols. The virus was diluted with sterile phosphate-buffered saline (PBS) to a final titer value of 5E + 8 TU/mL. The control vector that did not contain the target gene was used in the negative control (NC) group, and the titer was also 5E + 8 TU/mL. When cell confluence reached 20–30%, we transfected vectors into 6-10B cells. First, an inverted fluorescence microscope at magnification ×100 was used to evaluate the expression of the enhanced green fluorescent protein 3 days after transfection to determine the transfection efficiency. Thereafter, reverse transcription quantitative polymerase chain reaction (RT–qPCR) and western blot analysis were used to verify the mRNA and protein expression in the control vector (NC group)-treated, CSF-1R overexpression vector (transfection group)-treated, and untreated 6-10B cells.

2.3 | Reverse transcription-quantitative polymerase chain reaction

Total RNA was extracted from frozen tissues or cells using TRIzol reagent (Ambion; Thermo Fisher Scientific) following the manufacturer's protocol. Single-stranded cDNA was generated using a FastQuant RT kit (Tiangen Biotech, Beijing, China) following standard protocols at 42°C/15 min, 95°C/3 min, and 4°C/10 min. Next, 100 ng total cDNA was added per 25 μL reaction mixture with primers, and a SuperReal PreMix Plus SYBR Green PCR kit (Tiangen Biotech) was used to carry out the qPCR analysis. PCR was carried out using the following reaction conditions: 95°C/15 min, 95°C/10 s (40 cycles), and 60°C/32 s. Data were analyzed using the comparative ΔCt method with glyceraldehyde 3-phosphate dehydrogenase (GAPDH) as an internal normalization control.

Primers used in the study were mentioned in Table 1.

2.4 | Western blot analysis

Protein samples were prepared either from the cancerous tissues of nude mice or the cells. Tissues or cells were harvested and lysed in lysis buffer (Beyotime Institute of Biotechnology, Haimen, China), containing a protease inhibitor cocktail (100:1) and then kept on ice

TABLE 1 Quantitative polymerase chain reaction primers

Human CSF-1R forward	5′-TCTGGTCCTATGGCATCCTC-3′
Human CSF-1R reverse	5′-GATGCCAGGGTAGGGATTC-3′
GAPDH forward	5′-AGCCACATCGCTCAGACAC-3′
GAPDH reverse	5′-GCCCAATACGACCAAATCC-3′

CSF-1R, colony-stimulating factor-1 receptor; GAPDH, glyceraldehyde 3-phosphate dehydrogenase.

for ~30 min. Lysed tissues or cells were centrifuged at 12 000 *g* for 20 min at 4°C to remove cell debris. Total protein was extracted from the supernatant, and the concentration was estimated using a bicinchoninic acid assay kit (Beyotime Institute of Biotechnology). Proteins were separated on 10% sodium dodecyl sulphate-polyacrylamide gel electrophoresis and transferred onto nitrocellulose membranes. Membranes containing protein blots were incubated in blocking buffer (5% non-fat milk) for 1 h at room temperature, followed by overnight incubation at 4°C with the following primary antibodies: polyclonal rabbit anti-CSF-1R (dilution, 1:1000; catalogue no. 3152; Cell Signaling Technology, Danvers, MA, USA), monoclonal rabbit anti-cyclin D1 (dilution, 1:1000; catalog no. ab134175; Abcam, Cambridge, UK), monoclonal rabbit anti-Bcl-2 (dilution, 1:1000; catalog no. 4223; Cell Signaling Technology), monoclonal rabbit anti-Bax (dilution, 1:2000; catalog no. ab32124; Abcam), monoclonal rabbit anti-matrix metalloproteinase 2 (dilution, 1:2000; catalog no. ab92536; Abcam), monoclonal rabbit anti-beclin 1 (dilution, 1:1000; catalog no. 3495; Cell Signaling Technology), polyclonal rabbit anti-P62 (dilution, 1:1000; catalog no. 5114; Cell Technology), monoclonal rabbit anti-microtubule-associated protein 1 light chain 3 alpha (LC3; dilution, 1:1000; catalog no. 12741; Cell Signaling Technology), monoclonal rabbit anti-mTor (dilution, 1:1000; catalog no. 2983; Cell Signaling Technology), monoclonal rabbit anti-PI3K (dilution, 1:1000; catalog no. 3358; Cell Signaling Technology), monoclonal rabbit anti-Akt (dilution, 1:1000; catalog no. 9272; Cell Signaling Technology), monoclonal rabbit anti-phosphorylated (p)-Akt (dilution, 1:2000; catalog no. 4060; Cell Signaling Technology), and monoclonal rabbit anti-GAPDH (dilution, 1:1000; catalog no. ab181602; Abcam). The next day, membranes were thoroughly washed in 1 × TBST and incubated with HRP-conjugated mouse immunoglobulin, which was used as the secondary antibody (dilution, 1:3000; catalog no. 7074; Cell Signaling Technology) for 1.5 h at 37°C. Post-TBST washes of the membrane, protein signals were detected using an electrochemiluminescence kit (Pierce; Thermo Fisher Scientific). Densitometric quantification of the bands was carried out using ImageJ software (NIH, Bethesda, MD, USA).

2.5 | *In vivo* tumor growth assay

Three groups of 4-week-old nude mice were used. 6-10B cells, 6-10B cells with an empty vector, and 6-10B cells stably transfected with CSF-1R (1×10^6 cells suspended in 200 μL of PBS) were injected subcutaneously into the right dorsal flanks of nude mice. After the tumor mass appeared, its length and width were measured every 3 days using a microcaliper. The tumor volume (mm^3) was calculated using the equation: volume = length × $width^2$ / 2. Three weeks after injection, mice were killed by cervical dislocation. All the tumor tissues were weighed before fixation in 4% paraformaldehyde and embedded in paraffin, followed by the preparation of the sections for immunohistochemical (IHC) analyses. All animal experiments were reviewed and approved by the Institutional Animal Care and Use Committee of the People's Hospital of Guangxi Zhuang Autonomous Region.

2.6 | Immunohistochemical staining

The samples of excised tumor tissues from nude mice that were fixed in 4% paraformaldehyde, embedded in paraffin, and sectioned into 4-μm slices were used for IHC staining. The sections were dewaxed for 2 h in a 60°C incubator. Dewaxing and alcohol dehydration was carried out in the following order: xylene I, xylene II, xylene III, xylene IV, absolute ethyl alcohol, 95% ethyl alcohol, 80% ethyl alcohol, and 70% ethyl alcohol. Antigen retrieval was carried out by boiling the slides in citrate buffer solution for 20 min, followed by cooling them to room temperature. The sections were then incubated in 3% H_2O_2 for 20 min to prevent endogenous peroxidase activity, washed three times with PBS, and then incubated in sheep serum for 20 min. The sections were incubated at 4°C overnight with a rabbit anti-human CSF-1R monoclonal antibody (dilution, 1:100; catalogue no. ab183316; Abcam). The next day, the sections were warmed to room temperature for 2 h, washed three times with PBS, and incubated with a polymeric HRP-labeled anti-rabbit immunoglobulin G for 20 min. The slices were further washed three times with PBS and incubated with HRP-labeled streptomycin anti-biotin antibody for 20 min. The sections were subjected to three washes and followed by color development with 3,3′-diaminobenzidine. The sections were finally washed with water, and the cell nuclei were dyed using hematoxylin to facilitate observation under the light microscope.

2.7 | Statistical analysis

The data obtained were from at least three independent experiments, and all statistical analyses were carried out using GraphPad version 7.0 software (GraphPad, La Jolla, CA, USA). Data are presented as the mean ± standard deviation. Student's *t*-test was used to compare the diversity between two groups, and the four table χ^2-test or *t*-test was used to analyze categorical variables. The statistical significance was defined as $P < 0.05$.

3 | RESULTS

3.1 | Overexpression of CSF-1R in 6-10B cells

After transfecting the CSF-1R overexpressing vector into 6-10B cells, the transfection efficiency was analyzed by inverted fluorescence microscopy (Figure 1a). Green fluorescence was observed in the experimental transfection group and the NC group. RT–qPCR analysis showed that the mRNA expression of CSF-1R in the transfection group

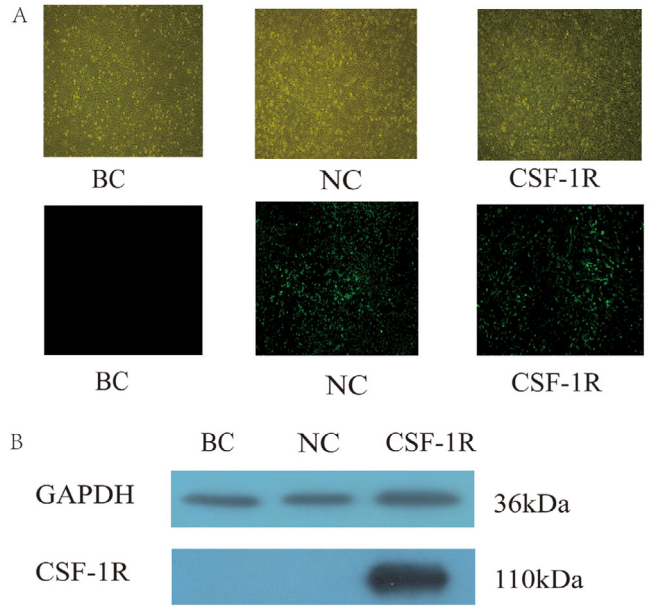

FIGURE 1 Overexpression of colony-stimulating factor-1 receptor (CSF-1R) in 6-10B cells. BC, blank control; GAPDH, glyceraldehyde 3-phosphate dehydrogenase; NC, negative control

was up to 9.435 ± 0.952, the blank control group was 0.777 ± 0.526, and the NC group was 0.933 ± 0.075. The difference was statistically significant ($F = 286.705$, $P < 0.001$). The protein expression of CSF-1R in blank control, NC, and experimental groups were 0.022 ± 0.004, 0.023 ± 0.004, and 1.925 ± 0.031, respectively (Figure 1b). The difference was statistically significant ($F = 11183.462$, $P < 0.001$).

3.2 | Effect of CSF-1R overexpression in 6-10B cells on tumor growth *in vivo*

To test whether CSF-1R played an important role *in vivo*, we used a xenograft mouse model. The tumorigenicity of 6-10B cells after transfection was compared with the mock group and the NC group in the nude mice model. Each mouse was inoculated with 2×10^6 cells. Five days post-inoculation, tumors were noted in the three groups of inoculated mice. Initially, we only observed a small white pit of the inoculation site, while the tumor gradually turned into a solid soft nodule, and the formation rate increased to 100% (Figure 2a). Subsequently, the length and width of the tumors were measured every 3 days using microcalipers (Table 2). Finally, the mice in each group were killed 3 weeks post-inoculation because of the large tumor size in the experimental group (Figure 2b).

The volume of tumors in the blank control and the NC groups were 96.152 ± 40.749 mm^3 and 297.943 ± 86.802 mm^3, respectively, whereas the volume of tumors in the transfection group was 1071.747 ± 214.399 mm^3 ($F = 72.119$, $P < 0.001$). The average quality of tumors formed by CSF-1R transfected cells was higher than that of other groups (Figure 2b). The mass of transplanted tumors in the blank control, NC, and transfection groups were 0.17 ± 0.11 g, 0 432 ± 0.156 g, and 2.406 ± 0.348 g, respectively ($F = 141.852$, $P < 0.001$). Hematoxylin–eosin staining (Figure 3a) and IHC analysis

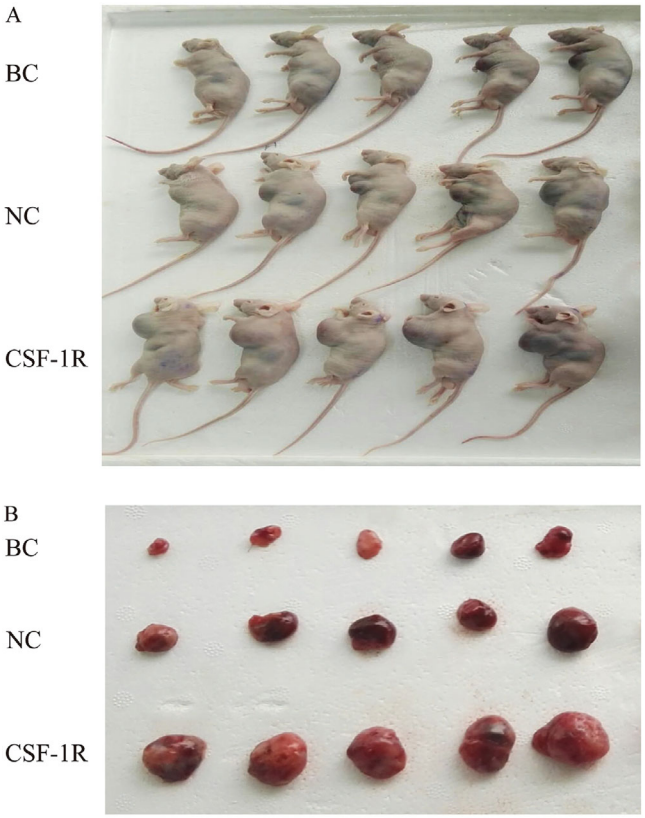

FIGURE 2 Colony-stimulating factor-1 receptor (CSF-1R) increased tumor growth *in vivo*. BC, blank control; NC, negative control

(Figure 3b) showed that CSF-1R was overexpressed in the experimental group.

3.3 | mRNA expression level of CSF-1R

The RT–PCR method showed that the relative expression of CSF-1R mRNA in the experimental group was 6.161 ± 0.319, which was significantly higher than that of the NC and blank control groups at 0.119 ± 0.100 and 0.076 ± 0.044, respectively. The values and differences were statistically significant ($F = 970.046$, $P < 0.001$).

3.4 | CSF-1R protein expression

As shown in Figure 4, the relative expression of CSF-1R in the blank control group was 0.023 ± 0.009, whereas that in the NC group and experimental transfection group was 0.025 ± 0.009 and 1.711 ± 0.201, respectively. Thus, the experimental protein expression was significantly higher as compared with that in the other groups ($F = 210.049$, $P = 0.013$).

3.5 | Expression of related proteins in nude mice xenografts

The relative expression levels of cyclin D1 in the blank control, NC, and experimental groups were 0.748 ± 0.163, 0.778 ± 0.150, and

TABLE 2 Volume changes of nude mice xenografts

Group	Day 6	Day 9	Day 12	Day 15	Day 18	Day 21
CSF-1R	71.471 ± 28.276*,#	113.749 ± 109.502*,#	209.000 ± 116.053*,#	422.006 ± 176.431*,#	702.214 ± 407.225*,#	1071.748 ± 214.400*,#
NC	7.107 ± 14.081	5.247 ± 0.702	14.497 ± 14.663	23.245 ± 14.405	57.230 ± 41.697	297.943 ± 86.802
BC	0.475 ± 1.062	22.595 ± 38.928	4.691 ± 6.790	8.637 ± 5.942	34.384 ± 17.701	96.152 ± 40.749

Data presented as the mean ± SD in mm^3 ($n = 5$).
*$P < 0.05$ compared with the mock group.
#$P < 0.05$ compared with the negative control (NC) group. BC, blank control; CSF-1R, colony-stimulating factor-1 receptor.

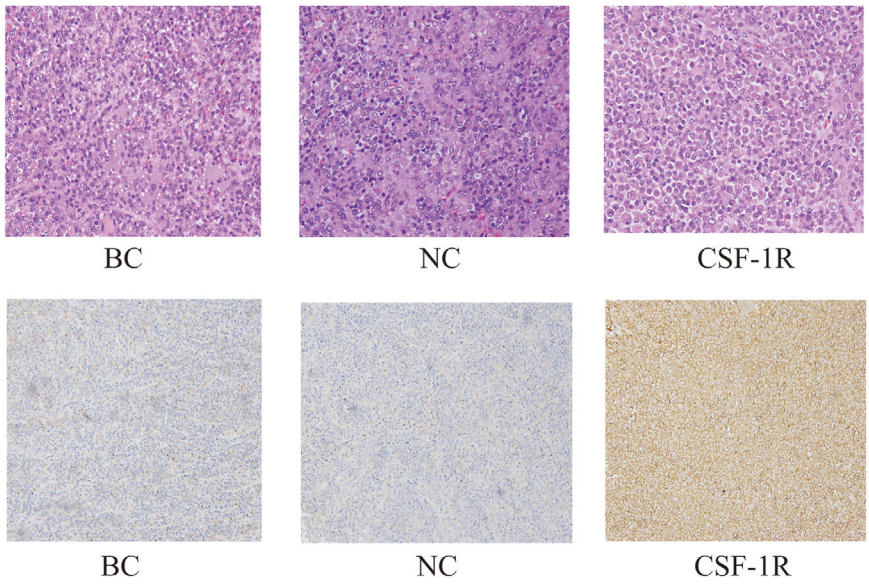

FIGURE 3 Pathological comparison of transplanted tumors in nude mice. BC, blank control; CSF-1R, colony-stimulating factor-1 receptor; NC, negative control

1.253 ± 0.123, respectively. The experimental group showed an upregulation ($F = 11.269$, $P = 0.009$). The expression level of the metastasis-associated protein matrix metalloproteinase 2 was 1.080 ± 0.051 in the experimental group, which was higher than that in the blank control (0.067 ± 0.012) and NC groups (0.422 ± 0.056; $F = 404.710$, $P < 0.001$). The apoptosis-related protein detection showed that the blank control and NC group Bax level was 0. 842 ± 0.124 and 0.703 ± 0.068, whereas that in the experimental group was 0.361 ± 0.093 ($F = 19.210$, $P = 0.002$). The Bcl-2 levels in blank control and NC groups were 0.013 ± 0.006 and 0. 034 ± 0.016, respectively, whereas those in the experimental group were 0.911 ± 0.141 ($F = 117.257$, $P < 0.001$). The expression level of autophagy protein beclin 1 in blank control, NC, and experimental groups was 0.268 ± 0.013, 0.322 ± 0.056, and 0.582 ± 0.035, respectively. The difference between the three groups was statistically significant ($F = 55.480$, $P < 0.001$). The relative expression of p62 in the three groups was 0.822 ± 0.151, 0.771 ± 0.108, and 0.406 ± 0.094, respectively, with a significant difference ($F = 10.673$, $P = 0.011$). The three groups had LC3 I/LC3 II levels at 8.343 ± 0.342, 4.221 ± 0.574, and 1.935 ± 0.318, respectively. The difference was statistically significant ($F = 173. 304$, $P < 0.001$). To sum up, the expression of cyclin D1, Bcl-2 and beclin 1 was upregulated, whereas that of LC3 I/LC3 II, Bax, and p62 was downregulated, and the differences were statistically significant. Overexpression of CSF-1R promotes autophagy, inhibits cell apoptosis, and increases proliferation. The PI3K/Akt/mTOR signaling pathway results are presented in Figure 4. The PI3K expression in the experimental group increased to 1.100 ± 0.096, the blank control was 0.068 ± 0.016, and the NC group was 0. 075 ± 0.020 ($F = 320.004$, $P < 0.001$). Akt of the blank control group was 0.505 ± 0.052, and the NC group was 0.613 ± 0.146, which was lower than the experimental group (0.948 ± 0.011; $F = 19.836$, $P = 0.002$). Phosphorylated Akt in the blank control group was 0.242 ± 0.106, and in the NC group was 0.530 ± 0.026, whereas the p-Akt in the experimental group was 0.960 ± 0.056 ($F = 78.401$, $P < 0.001$). The relative expression levels of the three groups of mTOR proteins were 0.620 ± 0.073, 0.631 ± 0.061, and 0.842 ± 0.058 respectively ($F = 11.333$, $P = 0.009$). Taken together, it is evident from these results that the overexpression of CSF-1R promotes the upregulation of PI3K, phosphorylated Akt, Akt, and mTOR, and activates the PI3K/Akt/mTOR signaling pathway.

4 | DISCUSSION

Apoptosis and autophagy are important physiological and pathological features of eukaryotes. They play a vital role in the normal growth and development, and are closely associated with the occurrence, establishment, and progression of a disease. Although both the processes show significant differences in the morphological features at the cellular level, signaling pathways, and biochemical metabolic pathways, they are potentially related. Apoptosis is typically characterized

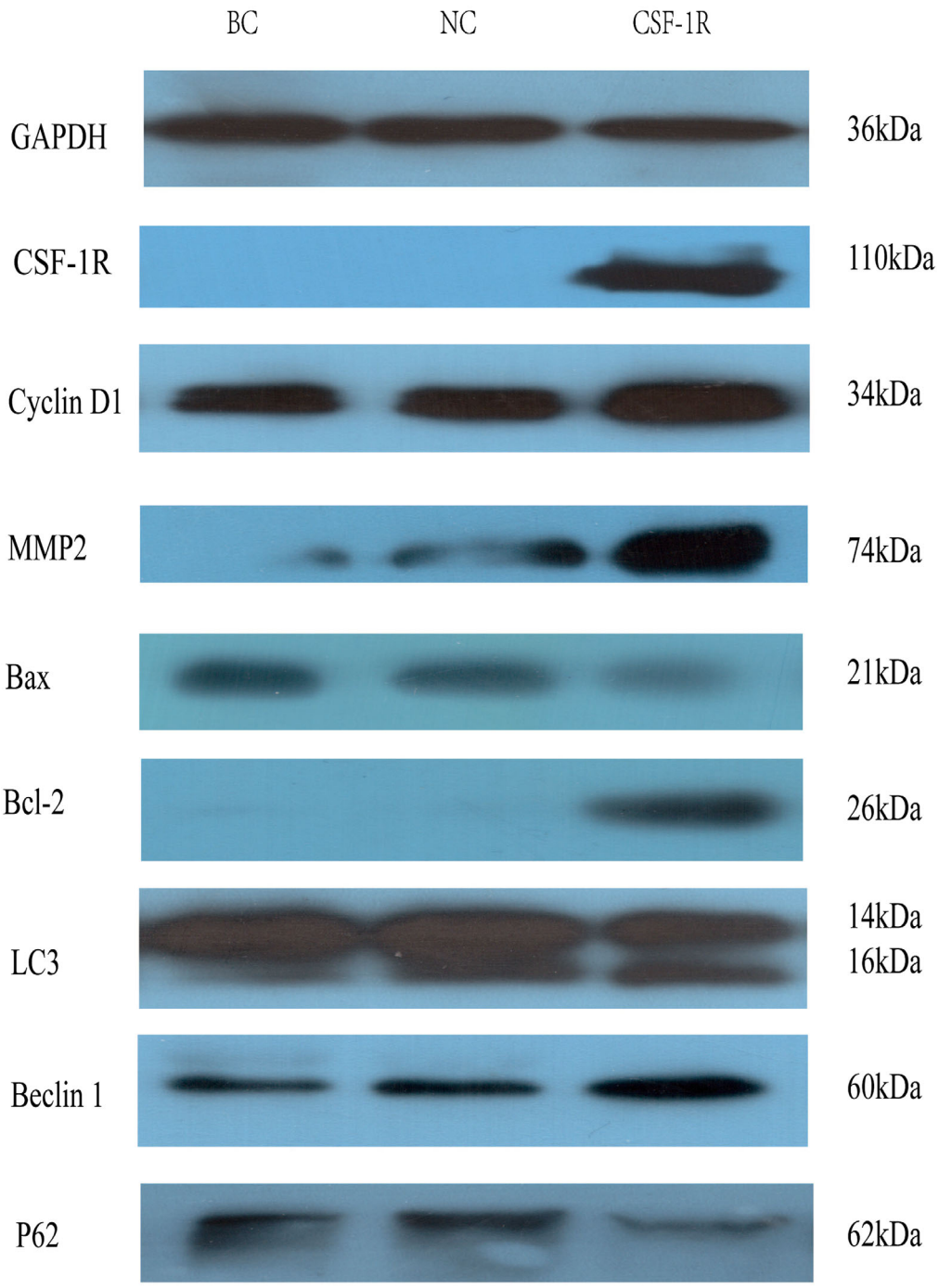

FIGURE 4 Western blot analyses of tumors of nude mice from each group. BC, blank control; CSF-1R, colony-stimulating factor-1 receptor; NC, negative control

by cytoplasmic shrinkage, nuclear condensation, DNA degradation, and the formation of apoptotic bodies. Residual cells are recognized, phagocytosed, and degraded by phagocytic cells. In contrast, autophagy is marked by the appearance of an autophagosome that encapsulates the cytoplasmic content of the bilayer membrane structure and fuses with the lysosomes to form autolysosomes. Autophagy has two complementary roles in determining cell fate. Although the overactivation of autophagy can cause cell death, autophagy can also be used as a self-rescuing act by the cells under certain pathological conditions, such as hunger, growth factor deprivation, hypoxia-ischemia, and so on. The regulation of both autophagy and apoptosis involves various regulatory factors, and hence, there appears to be a potential link between autophagy and apoptosis.

Previous studies have confirmed that the upregulation of cyclin D1 results in the cells losing their dependence on growth factors and loss of control on the regulation of the G1/S checkpoint. This triggers the cells into a continuous cell proliferation cycle, resulting in malignant proliferation and canceration.[11] Therefore, we believe that

overexpression of CSF-1R can promote the proliferation/progression of NPC.

Bcl-2 is proto-oncogene with a reported anti-apoptotic activity, and inhibits apoptosis in the downstream effector molecules of the Akt pathway. The presence of Bcl-2 in the mitochondria of NPC tissue exerts an anti-apoptotic effect by changing the permeability of the mitochondrial membrane, thereby preventing the release of cytochrome C. Conversely, Bax interacts with Bcl-2 on the mitochondrial membrane to form a heterodimer. This facilitates the formation of pore complex that penetrates the mitochondrial membrane, resulting in a reduction of the transmembrane potential, leading to cytochrome C leakage, and ultimately activating apoptosis. Furthermore, Bax and Bcl-2 are among the most important apoptosis regulators in the cells. The relative proportion of the two is a key factor in controlling cellular apoptosis.[12] The Bcl-2 to Bax (Bcl-2/Bax) ratio also serves as a marker for clinical tumor prognosis. The present study found that overexpression of CSF-1R can upregulate the Bcl-2/Bax ratio and inhibit apoptosis.

Beclin 1 is an important regulator of autophagy initiation and binds to PI3K to form the Atg1/ULK1 complex. This complex is regulated by mTOR. Akt directly phosphorylates PRAS40, which disables mTORC1 inhibition and activates the mTORC1 pathway. When mammals have sufficient energy in the body, mTORC is activated, and rapamycin target protein binds the autophagic complex and inhibits autophagy by inhibiting the activity of beclin 1. While the cellular energy levels are depleted, mTORC1 dissociates from the complex, releasing beclin 1 to induce autophagy.[13] LC3 is a homolog of the yeast autophagy-related gene 8 gene in mammalian cells, which targets the autophagic membrane and is involved in the execution of autophagy. LC3 is divided into type I and type II. When autophagy occurs, type I is modified by ubiquitin-like processing to bind phosphatidylethanolamine on the surface of autophagic membranes to form type II LC3 (lipidated LC3). LC3-II protein is located on intracellular autophagosome membranes, and is considered to be a marker for autophagosomes.[14] The LC3 levels measured in the present study corresponded to LC3-II protein levels. p62 protein encoded by the proto-oncogene c-Myc is localized in the nucleus, but is synthesized in the cytoplasm. When autophagy occurs, p62 in the cytoplasm first binds to ubiquitinated proteins, and then forms a complex with the LC3-II protein localized on the inner membrane; the complex is later degraded by autolysosomes. When autophagy occurs, the level of p62 decreases; however, p62 levels accumulate when autophagy activity is inhibited.[15] Therefore, it is speculated that overexpression of CSF-1R might promote autophagy in the nude mice injected with human NPC 6–10B cells.

Lin *et al*. described that capsaicin activates the PI3K/Akt/mTOR pathway, blocks the cell cycle G1 phase, and promotes autophagy and apoptosis by regulating the interaction between Bcl-2 and Beclin1 in NPC TW01 cells.[16] Similarly, Cheng *et al*. observed that overexpression of miR-185 can enhance apoptosis and autophagy, and prolong the survival time of patients with NPC.[17] Zheng *et al*. reported that the regulation of gossypol derivative ApoG2 can reduce the expression of Bcl-2, and promote apoptosis and autophagy in nasopharyngeal carcinoma CNE2 cells, thus inhibiting tumor growth.[18] Song *et al*. observed that autophagy is responsible for paclitaxel resistance seen in nasopharyngeal carcinoma cells.[19] Makowska *et al*.[20] found that the autophagy levels of NPC cell CNE-2R are negatively correlated with apoptosis and radiation resistance.[21] Pang *et al*. believe that emodin methyl ether can induce the ROS/miR-27a/ZBTB10 signaling axis by targeting Sp, and induce apoptosis and autophagy in nasopharyngeal carcinoma cells.[22] Gao *et al*. confirmed that overexpression of miR-138-5p enhances the sensitivity of nasopharyngeal carcinoma cells to radiation by targeting EIF4-EBP1.[23] Although the aforementioned studies have explored the relationship between autophagy and apoptosis in nasopharyngeal carcinoma on cancer cell proliferation, tumor growth, and radiotherapy reactivity, the conclusions are still not uniform.

However, these observations are based on only one cell line. Future studies involving more cell lines and more clinical data are required to confirm these effects in NPC patients. In conclusion, the present study based on a nude mouse tumor xenograft model showed that CSF-1R promotes proliferation and autophagy, but inhibits apoptosis in 6-10B NPC cell lines. Possible underlying mechanisms might involve activation of the PI3K/Akt pathway. These findings provide a further understanding of the process of NPC development, and indicate that CSF-1R inhibitors might be an effective treatment for NPC.

ACKNOWLEDGMENTS

The authors thank the Laboratory Center of the People's Hospital of Guangxi Zhuang Autonomous Region (Guangxi, China) for providing technical assistance. They also thank Dr Musheng Zeng and his colleagues at Sun Yat-Sen University Cancer Center for providing the 6-10B cell line.

CONFLICT OF INTEREST

The authors declare that they have read the article and there are no competing interests.

ORCID

Zenan Chen https://orcid.org/0000-0001-8022-0801

REFERENCES

1. Zhang L, Huang Y, Hong S, et al. Gemcitabine plus cisplatin versus fluorouracil plus cisplatin in recurrent or metastatic nasopharyngeal carcinoma: a multicentre, randomised, open-label, phase 3 trial [J]. *Lancet North Am Ed*. 2016;388(10054):1883-1892.
2. Kim J, Kwon J, Kim M, et al. Low-dielectric-constant polyimide aerogel composite films with low water uptake [J]. *Polym J*. 2016;48(7):829-834.
3. Guo Y, Zhu XD, Qu S, et al. Identification of genes involved in radioresistance of nasopharyngeal carcinoma by integrating gene ontology and protein-protein interaction networks [J]. *Int J Oncol*. 2012;40(1):85-92.
4. Yang S, Chen J, Guo Y, et al. Identification of prognostic biomarkers for response to radiotherapy by DNA microarray in nasopharyngeal carcinoma patients [J]. *Int J Oncol*. 2012;40(5):1590-1600.

5. Torti D, Trusolino L, Oncogene addiction as a foundational rationale for targeted anti-cancer therapy: promises and perils [J]. *EMBO Mol Med*. 2011;3(11):623-636.
6. Kirma N, Hammes LS, Liu YG, et al. Elevated expression of the oncogene c-fms and its ligand, the macrophage colony-stimulating factor-1, in cervical cancer and the role of transforming growth factor-beta1 in inducing c-fms expression [J]. *Cancer Res*. 2007;67(5):1918-1926.
7. Baay M, Brouwer A, Pauwels P, et al. Tumor cells and tumor-associated macrophages: secreted proteins as potential targets for therapy [J]. *Clin Dev Immunol*. 2011;2011(565187).
8. Gruessner C, Gruessner A, Glaser K, et al. Biomarkers and endosalpingiosis in the ovarian and tubal microenvironment of women at high-risk for pelvic serous carcinoma.[J]. *Am J Cancer Res*. 2014;4(1):61-72.
9. Aligeti S, Kirma NB, Binkley PA, et al. Colony-stimulating factor-1 exerts direct effects on the proliferation and invasiveness of endometrial epithelial cells [J]. *Fertil Steril*. 2011;95(8):2464-2466.
10. Chen J, Hao Y, Chen J, et al. Colony stimulating factor-1 receptor promotes proliferation, migration and invasion in the human nasopharyngeal carcinoma 6–10b cell line via the phosphoinositide 3-kinase/akt pathway [J]. *Oncol Lett*. 2018;16(1):1205-1211.
11. Shan BE, Wang MX, Li RQ, Quercetin inhibit human sw480 colon cancer growth in association with inhibition of cyclin d1 and survivin expression through wnt/beta-catenin signaling pathway [J]. *Cancer Invest*. 2009;27(6):604-612.
12. Tomasin R, Gomes-Marcondes MC, Oral administration of aloe vera and honey reduces walker tumour growth by decreasing cell proliferation and increasing apoptosis in tumour tissue [J]. *Phytother Res*. 2011;25(4):619-623.
13. Jung CH, Ro SH, Cao J, et al. Mtor regulation of autophagy [J]. *FEBS Lett*. 2010;584(7):1287-1295.
14. Mathew R, Karp CM, Beaudoin B, et al. Autophagy suppresses tumorigenesis through elimination of p62 [J]. *Cell*. 2009;137(6):1062-1075.
15. Gozuacik D, Kimchi A, Autophagy as a cell death and tumor suppressor mechanism [J]. *Oncogene*. 2004;23(16):2891-2906.
16. Lin YT, Wang HC, Hsu YC, et al. Capsaicin induces autophagy and apoptosis in human nasopharyngeal carcinoma cells by downregulating the pi3k/akt/mtor pathway [J]. *Int J Mol Sci*. 2017;18(7).
17. Cheng JZ, Chen JJ, Wang ZG, et al. Microrna-185 inhibits cell proliferation while promoting apoptosis and autophagy through negative regulation of tgf-beta1/mtor axis and hoxc6 in nasopharyngeal carcinoma [J]. *Cancer Biomark*. 2018;23(1):107-123.
18. Zheng R, Chen K, Zhang Y, et al. Apogossypolone induces apoptosis and autophagy in nasopharyngeal carcinoma cells in an in vitro and in vivo study [J]. *Oncol Lett*. 2017;14(1):751-757.
19. Song Y, Li W, Peng X, et al. Inhibition of autophagy results in a reversal of taxol resistance in nasopharyngeal carcinoma by enhancing taxol-induced caspase-dependent apoptosis [J]. *Am J Transl Res*. 2017;9(4):1934-1942.
20. Makowska A, Eble M, Prescher K, et al. Chloroquine sensitizes nasopharyngeal carcinoma cells but not nasoepithelial cells to irradiation by blocking autophagy [J]. *PLoS One*. 2016;11(11):e0166766.
21. Liang ZG, Lin GX, Yu BB, et al. The role of autophagy in the radiosensitivity of the radioresistant human nasopharyngeal carcinoma cell line cne-2r [J]. *Cancer Manag Res*. 2018;10:4125-4134.
22. Pang MJ, Yang Z, Zhang XL, et al. Physcion, a naturally occurring anthraquinone derivative, induces apoptosis and autophagy in human nasopharyngeal carcinoma [J]. *Acta Pharmacol Sin*. 2016;37(12):1623-1640.
23. Gao W, Lam JW, Li JZ, et al. Microrna-138-5p controls sensitivity of nasopharyngeal carcinoma to radiation by targeting eif4ebp1 [J]. *Oncol Rep*. 2017;37(2):913-920.

How to cite this article: Chen Z, Hao Y. Effect of colony-stimulating factor-1 receptor overexpression on the growth of nasopharyngeal carcinoma xenografts in nude mice and its mechanism of action. *Prec Radiat Oncol*. 2020;4:10–17. https://doi.org/10.1002/pro6.1078